

Manuscript Number:

Title: THE TARAKLI FLYSCH IN THE BOYALI AREA (SAKARYA TERRANE, NORTHERN TURKEY):  
IMPLICATIONS FOR THE TECTONIC HISTORY OF THE INTRAPONTIDE SUTURE ZONE

Article Type: Full Length Article / Article original

Section/Category: TECTONIQUE / TECTONICS

Keywords: Foredeep deposits; Sakarya Terrane; IntraPontide suture zone; Tarakli Flysch; Northern Turkey.

Corresponding Author: PROF. MICHELE MARRONI, Ph.D.

Corresponding Author's Institution: UNIVERSITY OF PISA

First Author: MICHELE MARRONI, Ph.D.

Order of Authors: MICHELE MARRONI, Ph.D.; RITA CATANZARITI; ELLERO ALESSANDRO; M.CEMAL GÖNCÜOĞLU; MICHELE MARRONI; GIUSEPPE OTTRIA

Abstract: In the Boyali area, Northern Turkey, the tectonic units of the Istanbul-Zonguldak Terrane and the IntraPontide suture zone are thrust over the deposits at the top of the Sakarya Terrane, known as Tarakli Flysch. It consists of Early Maastrichtian-Middle Paleocene turbidite and mass-gravity deposits, whose source mainly corresponds to the Istanbul-Zonguldak Terrane, and with a lesser extent, to the IntraPontide suture zone. These deposits were sedimented in a foredeep basin developed during the convergence between Sakarya and Eurasian continental microplates. In the Late Paleocene-Early Eocene time span, the Tarakli Flysch was deformed (D1 phase) during the closure of the foredeep basin. In the Miocene time, the strike-slip tectonics (D2 phase) related to the North Anatolian fault produced further deformations of the Tarakli Flysch.

Suggested Reviewers: ARAL OKAY  
okay@itu.edu.tr  
Researcher expert in regional geology of Turkey

OKAN TUYSUZ  
tuysuz@itu.edu.tr  
Researcher expert in regional geology of Turkey

Opposed Reviewers:

1  
2  
3  
4 **THE TARAKLI FLYSCH IN THE BOYALI AREA (SAKARYA**  
5 **TERRANE, NORTHERN TURKEY): IMPLICATIONS FOR THE**  
6 **TECTONIC HISTORY OF THE INTRAPONTIDE SUTURE ZONE**  
7  
8  
9

10  
11  
12 **LE FLYSCH DE TARAKLI DANS LA ZONE DE BOYALI (SAKARYA TERRANE,**  
13 **NORD DE LA TURQUIE): CONSÉQUENCES POUR L'HISTOIRE TECTONIQUE DE**  
14 **LA ZONE DE SUTURE INTRAPONTIDE**  
15  
16  
17  
18  
19

20 Rita Catanzariti<sup>a</sup>, Alessandro Ellero<sup>a</sup>, M. Cemal Göncüoğlu<sup>b</sup>, Michele Marroni<sup>c,a</sup>,  
21 Giuseppe Ottria<sup>a</sup>, Luca Pandolfi<sup>c,a</sup>,  
22  
23  
24  
25  
26  
27  
28

29 a Istituto di Geoscienze e Georisorse, CNR, Pisa, Italy

30 b Department of Geological Engineering, Middle East Technical University, Ankara,  
31 Turkey  
32

33 c Dipartimento di Scienze della Terra, Università di Pisa, Italy  
34  
35  
36  
37  
38  
39  
40  
41  
42  
43

44 =====  
45  
46 CORRESPONDING AUTHOR:

47 PROF. MICHELE MARRONI,

48 DIPARTIMENTO DI SCIENZE DELLA TERRA,

49 UNIVERSITÀ DI PISA, VIA S. MARIA, 53

50 56126 PISA, ITALY.

51 E-MAIL: [marroni@dst.unipi.it](mailto:marroni@dst.unipi.it)  
52  
53  
54  
55  
56  
57  
58  
59  
60  
61  
62  
63  
64  
65

1  
2  
3  
4 ABSTRACT  
5

6 In the Boyali area, Northern Turkey, the tectonic units of the Istanbul-Zonguldak Terrane  
7 and the IntraPontide suture zone are thrust over the deposits at the top of the Sakarya  
8 Terrane, known as Tarakli Flysch. It consists of Early Maastrichtian-Middle Paleocene  
9 turbidite and mass-gravity deposits, whose source mainly corresponds to the Istanbul-  
10 Zonguldak Terrane, and with a lesser extent, to the IntraPontide suture zone. These  
11 deposits were sedimented in a foredeep basin developed during the convergence between  
12 Sakarya and Eurasian continental microplates. In the Late Paleocene-Early Eocene time  
13 span, the Tarakli Flysch was deformed (D1 phase) during the closure of the foredeep  
14 basin. In the Miocene time, the strike-slip tectonics (D2 phase) related to the North  
15 Anatolian fault produced further deformations of the Tarakli Flysch.  
16  
17  
18  
19  
20  
21  
22  
23

24 RESUME'  
25

26 Dans la zone de Boyali, nord de la Turquie, les unités tectoniques du terrane Istanbul-  
27 Zonguldak et de la zone de suture IntraPontide sont chevauchée sur les dépôts au sommet  
28 du terrane de Sakarya, connu sous le nom de Flysch de Tarakli. Il se compose de  
29 turbidites et des dépôts de glissement en masse sous-marine d'âge Maastrichtien-  
30 Paléocène moyenne, dont la source correspond principalement à la terrane Istanbul-  
31 Zonguldak, et dans une moindre mesure, à la zone de suture IntraPontide. Ces dépôts ont  
32 été sédimentées dans un bassin avant-fosse développée au cours de la convergence entre  
33 les microplaques continentales Sakarya et Eurasia. Dans le Paléocène-Eocène Inferieure,  
34 le Flysch Tarakli a été déformé (phase D1) lors de la fermeture du bassin avant-fosse.  
35 Dans le Miocène, la tectonique décrochement (phase D2) liée à la faille Nord Anatolienne  
36 produit déformations en outre de Flysch Tarakli.  
37  
38  
39  
40  
41  
42  
43  
44

45  
46 KEY WORDS: Foredeep deposits, Sakarya Terrane, IntraPontide suture zone, Tarakli  
47 Flysch, Northern Turkey.  
48  
49

50  
51 E-mail addresses: Rita Catanzariti (catanzariti@igg.cnr.it), Alessandro Ellero  
52 (ellero@igg.cnr.it), M. Cemal Göncüoglu (mcgoncu@metu.edu.tr), Michele Marroni  
53 (marroni@dst.unipi.it), Giuseppe Ottria (ottria@dst.unipi.it), Luca Pandolfi  
54 (pandolfi@dst.unipi.it),  
55  
56  
57  
58  
59  
60  
61  
62  
63  
64  
65

1  
2  
3  
4 **1. Introduction**  
5  
6

7  
8 The present-day tectonic setting of the Turkey can be depicted as a giant geological  
9 puzzle represented by amalgamated continental microplates separated by ophiolite-  
10 bearing suture zones, whose ages range from Late Neoproterozoic to Cretaceous (e.g.,  
11 Göncüoğlu et al, 1997 and quoted references). One of the most important but still poorly  
12 studied suture zones of Northern Turkey is represented by the IntraPontide one,  
13 originated from the continental collision between the Sakarya (hereafter SK) and Eurasian  
14 Istanbul-Zonguldak (hereafter IZ) microplates. The tectonic units of IntraPontide Suture  
15 (hereafter IPS) zone are thrust over the Tarakli Flysch, i.e. a turbidite succession  
16 representing the sedimentary cover of SK Terrane.  
17  
18

19 Thus, the detailed analysis focused on the Tarakli Flysch may provide useful insights  
20 for the reconstruction of the IPS zone.  
21  
22

23 In this paper, an integrate study of the stratigraphical, paleontological and structural  
24 features of the Tarakli Flysch cropping out in the Boyali area, Northern Turkey, is  
25 presented and the implications for the tectono-sedimentary evolution of the IPS zone are  
26 discussed.  
27  
28  
29  
30  
31  
32

33 **2. Geological Setting**  
34  
35  
36

37 In Northern Turkey (Fig.1), the IPS zone (Robertson and Ustaömer, 2004, Göncüoğlu  
38 et al., 2008) separates the IZ Terrane (Saribudak et al., 1989), in the north, from the SK  
39 Terrane of Gondwana affinity, in the south. Whereas the IZ Terrane is regarded as  
40 belonging to Eurasia plate, the SK Terrane is interpreted as representative of the SK  
41 microplate, separated from the Eurasia continental margin by the IPS oceanic basin.  
42  
43  
44

45 The IPS zone is regarded as originated by the Late Cretaceous to Early Tertiary  
46 convergence between IZ and SK plates, leading to complete destruction of the oceanic  
47 basin. The remnants of this basin are preserved in the IPS zone, where an imbricate stack  
48 of oceanic and continental units have been detected along its whole extent.  
49  
50  
51

52 The IZ Terrane includes a Late Neoproterozoic basement (e.g., Ustaömer and Rogers,  
53 1999) unconformably covered by a continuous, well-developed sedimentary sequence  
54 ranging in age from Ordovician to Carboniferous, only mildly deformed during the  
55 Variscan orogeny (e.g., Gorur et al., 1997). The non-metamorphic Paleozoic sequence of  
56 the IZ Terrane is unconformably overlain by Late Permian-earliest Triassic sedimentary  
57  
58  
59  
60  
61  
62  
63  
64  
65

1  
2  
3  
4 rocks, and their transition to turbidite deposits of Late Triassic age. The Triassic rocks are  
5 unconformably overlain by Late Cretaceous–Paleocene turbidite deposits (Akveren  
6 Flysch) where andesitic volcanic rocks have been found (e.g., Dizer and Meric, 1983).  
7 Senonian andesitic lavas, dikes, and small acidic intrusions are the witness of a north-  
8 dipping subduction of the NeoTethys oceanic lithosphere below the continental crust of  
9 IZ Terrane.  
10  
11

12  
13  
14 The IPS units are thrust over the SK Unit derived from SK Terrane and represented, in  
15 the studied geotraverse, by the Karakaya Complex and its sedimentary cover. The  
16 Karakaya Complex represents the remnants of a Triassic accretionary wedge (Okay and  
17 Göncüoğlu, 2004 and quoted references), where metabasites and metaserpentinites are  
18 preserved (Sayit and Göncüoğlu, 2009). The lower Karakaya Complex was strongly  
19 deformed under a latest Triassic, high-pressure facies metamorphism (Okay et al., 2002),  
20 interpreted as the result of the Cimmerian orogenesis. The tectonic structures related to  
21 the Cimmerian orogeny are unconformably sealed by the continental- to shallow-marine  
22 Early Jurassic clastic rocks, in turn disconformably topped by the Middle Jurassic to  
23 Early Cretaceous neritic carbonates (Yigitbas et al, 1999). The neritic carbonates are  
24 unconformably overlain by the Albian–Cenomanian pelagic limestones showing a  
25 transition to turbidite deposits (here reported as Tarakli Flysch) ranging in age from Late  
26 Cretaceous to Paleocene.  
27  
28

29  
30 In the study area, along the geotraverse Kursunlu-Arac, the IPS zone can be defined as  
31 an imbricate stack of four types of tectonic units: the ophiolite units, the Arkotdag  
32 Mèlange, the High-Grade Metamorphic Unit and the Low-Grade Metamorphic Unit  
33 (Fig.1). The imbricate stack is probably the result of multiple event of thrusting leading to  
34 present-day juxtaposition of oceanic and continental units. These units are sandwiched  
35 between the IZ Terrane at the top and the SK Terrane at the bottom. The relationships of  
36 the rock-units of the IPS zone area sealed by sedimentary deposits of Early Eocene.  
37 Strike-slip tectonics related to the still active North-Anatolian Fault Zone (hereafter  
38 NAFZ) modified the original relationships among the rock-units of the IPS zone.  
39  
40  
41  
42  
43  
44  
45  
46  
47  
48  
49  
50  
51  
52

### 53 **3.The Tarakli Flysch in Boyali area**

54  
55

56 The study area corresponds to the E-W trending strip to the North of Kursunlu and  
57 Ilgaz along the Akçay and Boyalıçay valleys between the Aylı Mountain in the North and  
58 Gürgenli and Köklüce mountains in the South (Fig.2). In the Boyali area, even if their  
59  
60  
61  
62  
63  
64  
65

1  
2  
3  
4 relationships are reworked by strike-slip faults, the overthrust of the Arkotdag Mélange  
5 onto the Tarakli Flysch can be still identified in the field. Dykes of andesites cutting the  
6 Tarakli Flysch have been found.  
7  
8

### 9 *3.1. Stratigraphic features*

10 The stratigraphic features of the Tarakli Flysch have been fully reconstructed in the  
11 sections cropping out along the northern side of the Akçay Valley, between the Bahcecik  
12 and Boyali Villages and along the Boyalıçay Valley (Fig.2). The succession, whose  
13 thickness has been estimated as at least 700 m, shows a clear thickening and coarsening  
14 upward evolution that can be divided in five different lithofacies (see Fig. 3A log for  
15 more details) that, from the bottom to the top, are: "thin-bedded turbidites", "medium-  
16 grained arenites", "conglomerates", "calcareous coarse-grained turbidites" and "slide-  
17 block in shaly-matrix" lithofacies.  
18  
19

20 The lower most part of Tarakli Flysch is characterized by 400 m thick thin-bedded  
21 turbidites consisting of thin to medium beds (5-50 cm) of medium- to fine-grained  
22 arenites and coarse-grained siltites (Fig. 3B1). The medium- to fine-grained arenites are  
23 often characterized by thin traction carpets. These strata are generally well graded only in  
24 their uppermost part where current ripples and sinusoidal lamina can be also present. In  
25 the uppermost part of this lithofacies decimetric lenticular beds of coarse-grained arenites  
26 can be recognized (Fig.3B2).  
27  
28

29 The medium-grained arenites lithofacies is characterized by up to 50 m thick sequence  
30 of turbidites represented by 0.5-2.5 m thick beds of amalgamated medium- to fine-  
31 grained arenites alternating with subordinate thin beds of shales (Fig. 3A). These strata  
32 are characterized by the lack of sedimentary features as graded bedding and lamina and a  
33 quite massive structure can be recognized. The bottom surface of these strata is marked  
34 by sole marks and by the widespread presence of organic matter (leaves and tree cortex  
35 fragments).  
36  
37

38 A dm-thick level of well rounded clast- to matrix-supported conglomerates (Fig. 3B3)  
39 characterize the medium part of the Tarakli Flysch and represent, in this area, a key level  
40 to understand the geometry of the main structures. The most striking feature of this  
41 lithofacies is represented by granite-dominated composition of the pebbles. These beds,  
42 derived from high density erosive flows probably connected to a coarse-grained river-  
43 delta system, are characterized by frequent basal erosional features.  
44  
45

46 The calcareous coarse-grained turbidites lithofacies consist of a sequence of layers  
47 (not thicker than 25-30 m) ranging from clast-supported orthoconglomerates to coarse  
48  
49  
50  
51  
52  
53  
54  
55  
56  
57  
58  
59  
60  
61  
62  
63  
64  
65

1  
2  
3  
4 arenites mainly derived from debris flows and high density turbidity currents. The most  
5 common facies is represented by prevalent monomict clast-supported conglomerates  
6 characterized by poor sorting. The internal organization of these deposits, characterized  
7 by unsorted coarse clasts, is scarce. These beds, derived from high density erosive flows,  
8 are characterized by frequent basal erosional features. The erosional ability is suggested  
9 by frequent bottom bedset scours, diffuse amalgamated surfaces, and common rip-up mud  
10 clasts. These strata are associated with coarse-grained high density turbidity current  
11 deposits. Thick to medium beds without internal structures and with poor sorting are the  
12 most common facies. A subtle normal grading and water escape features can be  
13 recognized in a few beds.  
14  
15

16 The most prominent feature of these members is the quasi-monomict composition of  
17 the debris characterized by extrabasinal carbonatic clasts.  
18  
19

20 The upper part of the succession (up to 400 m thick) is dominated by huge slide-  
21 blocks embedded in a fine grained-matrix (Fig. 3B4). The matrix of this lithofacies is  
22 characterized by varicolored mainly shaly to silty deposits. Subordinate decimetric  
23 lenticular beds of coarse-grained arenites have been also recognized. The slide-blocks,  
24 usually with lenticular shapes, show different size (ranging from boulder up to 100 m-  
25 thick blocks) and composition. Even if the primary relationships between the slide blocks  
26 and the surrounding matrix are always tectonized, their emplacement due to submarine  
27 landslides for these blocks is suggested by synsedimentary deformation structures  
28 recognized in the sediments around the blocks and by slide block-derived monomict  
29 pebbly-mudstones and pebbly-sandstones that are present around several slide-blocks.  
30 The slide-blocks are mainly made up of granitoids, orthogneisses,  
31 metagabbros/amphibolites, Jurassic carbonatic turbidites next to Ordovician  
32 quartzarenites, black shales, crinoidal (Fig. 3B5) and brachiopod-bearing Devonian-  
33 Carboniferous limestones and probably Triassic red quartzarenites (Fig. 3B4) as typical  
34 representatives of the IZ Terrane. Few blocks of serpentinites have been also recognized  
35 in the uppermost part of the sequence.  
36  
37  
38  
39  
40  
41  
42  
43  
44  
45  
46  
47  
48  
49  
50  
51

### 52 *3.2. Arenite petrography*

53 35 thin sections from Tarakli Flysch (30 arenites and 5 rudites) were analyzed by  
54 means of polarizing microscope. A modal analysis was performed on 19 selected  
55 medium- to coarse-grained arenites. Point counting (500 points) of arenites was  
56 performed using the Gazzi-Dickinson technique (Zuffa, 1987 and quoted references) to  
57  
58  
59  
60  
61  
62  
63  
64  
65

1  
2  
3  
4 minimize the dependence of arenite composition on grain size. The point counting results  
5 are plotted on the triangular diagrams of Fig. 3C.  
6

7  
8 No large differences can be recognized in the framework composition of arenites from  
9 the Tarakli Flysch. They range from quartz-poor mixed arenites up to calcilithites. The  
10 total framework is characterized by a mixed siliciclastic-carbonate framework  
11 composition (Fig. 3C1) where the important carbonatic extrabasinal contribution (CE, up  
12 to the 50%) led to classified these rocks as mixed arenites (Zuffa, 1980).  
13  
14

15  
16 The extrabasinal siliciclastic framework is characterized by a common presence of  
17 mono- and polycrystalline quartz (12÷41% of the total framework) and feldspar (6÷31%).  
18 Felsic intrusive coarse-grained rock fragments, such as granitoids, are common (0÷3% of  
19 the total framework) while low grade metamorphic rock fragments are not common and  
20 include coarse-grained gneisses, metaquartzites, fine-grained schists and mica-schists  
21 (1÷8% of the total framework).  
22  
23

24  
25 A striking feature of the Tarakli Flysch arenites is the widespread presence of  
26 carbonate rock fragments (Fig. 3C1). In all the studied samples both intra- (1÷30% of the  
27 total framework) and extra-basinal (22÷48%) carbonate fragments have been recognized.  
28 Carbonate extrabasinal fragments are represented by carbonate platform derived rocks,  
29 mainly mudstones, wackestones and grainstones of Jurassic - Early Cretaceous age (Fig.  
30 3B6). The allochems in the grainstone fragments are peloids, ooids, minor benthic  
31 foraminifera and undeterminable macrofossil fragments. The intrabasinal carbonate  
32 fragments are instead represented by mudstone, showing deformed and squeezed soft  
33 margins and by isolated bioclasts, mainly benthic foraminifera and macrofossils (Fig.  
34 3B6). The presence of intrabasinal carbonate fragments became relevant in the calcareous  
35 coarse-grained turbidites. The arenites composition of this lithofacies indicate a strong  
36 supply from a coeval carbonate platform (up to 65% of the total framework, Fig. 3C1)  
37  
38  
39  
40  
41  
42  
43  
44

45  
46 The lacking of ophiolite-derived rock fragments, represents one of the more striking  
47 features of Tarakli Flysch arenites. Therefore the source areas of these sediments were  
48 mainly characterized by a continental basement made up of granitoids, metamorphic  
49 rocks, felsic volcanic rocks and the relative sedimentary covers, represented by  
50 extrabasinal non coeval carbonate rock successions.  
51  
52

53  
54 This source area can be related to a typical continental margin. The lithic fragments in  
55 the arenites debris and the composition of the main slide-blocks in the uppermost part of  
56 the succession seem to indicate the IZ Terrane as the most probable source area of the  
57 Tarakli Flysch.  
58  
59  
60  
61  
62  
63  
64  
65



### 3.3. Nannofossil analyses

55 samples were analyzed for the calcareous nannofossil study of the Tarakli Flysch. The analyses were performed on smear slides, prepared from unprocessed material, using a light microscope at 1250 magnification. The taxa have been recognized following the taxonomy proposed by Perch-Nielsen (1985a, 1985b) and Bown (1999). The investigated samples and the recognised calcareous nannofossil taxa are provided in Table A. Several samples (19) are barren, while the investigated assemblages suffered overgrowth and dissolution. However some informations about the age of the identified lithofacies have been obtained.

In the lowermost thin-bedded turbidites lithofacies, a sample with a monogeneric assemblage (ABT04), composed of common *Micula staurophora*, *Micula concava* and *Micula* sp., has been collected. This sample can be referred to the Maastrichtian on the basis of paleoclimatic consideration. The genus *Micula* is considered a cold water indicator and the genus *Watznaueria* is related to warm water condition. Bojar Melinte et al. (2009) record a *Watznaueria/Micula* cross over, in Early Maastrichtian, as a result of colder water condition. The monospecific assemblage of *Micula* spp. found in our sample could be related to this cold event and indirectly dated to the Early Maastrichtian. Reworking is evidenced by the sample ABT02 where the finding of *Ephrolithus floralis* indicates the Late Aptian-Late Cenomanian time interval. On the contrary, samples TC21 and TC22 from marls from of the shaly-matrix lithofacies around the slide-blocks have been dated to the Middle Paleocene (Selandian zone NP5 of Martini, 1971) on the occurrence of *Heliolithus cantabriae*, *Fasciculithus ulii*, *Fasciculithus tympaniformis* and *Sphenolithus anarrhopus*. The characteristics of this lithofacies resulted in a strong reworking of the nannofossil assemblages. For instance, the sample with *Polycostella beckmannii* and *Diazomatolithus lehmanii* (ABT22) can be referred to the *Polycostella beckmannii* Subzone (NJ20B) of Bralower et al. (1989) referable to the Middle Tithonian, and samples bearing *Nannoconus* sp., *Hexalithus noeliae*, *H. chiastia*, *P. beckmannii* and *D. lehmanii* (TC196, TC197, TC198) have been dated to the NJK Zone (Jurassic-Cretaceous boundary) of Bralower et al. (1989).

In summary, the nannofossil analyses indicate an Early Maastrichtian for the lowermost level of the studied succession, whereas a Middle Paleocene age can be proposed for its top, i.e. the slide-block in shaly-matrix lithofacies.

### 3.3. Deformation history

1  
2  
3  
4 The Tarakli Flysch is characterized by a complex deformation pattern, even if the  
5 whole succession is non-metamorphic. This deformation pattern is the result of two main  
6 deformation phases, referred as D1 and D2 phases, whose structures are well identifiable  
7 in the field.  
8  
9

10 The structures of the D1 phase are represented by F1 folds that commonly display a  
11 geometry ranging from isoclinal to subisoclinal. The F1 fold axes show from NW-SE to  
12 NNW-SSE strike with steep plunges (Fig.4A).  
13  
14

15 At the outcrop scale the F1 folds are overprinted by a cm- to tens of meter-scale  
16 structures (Fig.4A) represented by a complex association of faults, thrusts and folds, all  
17 referred to D2 phase (Fig. 4B and C).  
18  
19

20 The faults occur as high-angle brittle shear zones grouped into three main systems  
21 with E-W, NNW-SSE and NNE-SSW strike, respectively referred to S1, S2 and S3  
22 systems (Fig.4D). The faults of S1 and S3 systems show predominantly dextral strike-slip  
23 movements, but slip sense indicators of normal movements are also observed. On the  
24 contrary, the faults of S2 system are mainly represented by sinistral strike-slip faults. The  
25 thrusts are represented by flat shear zones with medium to low dip and NNW-SSE and  
26 ENE-WSW strike (Fig.4C). The thrusts are characterized by both northward and  
27 southwestward sense of shear. In the field, examples of structures where the thrusts are  
28 rooted into the high angle strike-slip faults are common.  
29  
30  
31  
32  
33  
34  
35

36 The F2 folds can be instead grouped into two main groups based on their geometry  
37 and/or relationships with faults and thrusts. The first type F2a corresponds to upright  
38 folds directly associated with steeply dipping faults (Fig.4B). Strike of fold axes and axial  
39 planes are roughly parallel to that of the related faults. These upright folds show hinge  
40 zone that may be partially cut out by the faults, whereas the vertical fold limbs are cut by  
41 an array of faults parallel to the bedding planes or cross-cutting at low angles to produce  
42 imbricate zones. The second type F2b includes the folds associated with the thrusts. The  
43 F2b folds display sub-horizontal axes and axial planes, whose strikes is roughly parallel  
44 to the mean directions of the thrusts (Fig.4C).  
45  
46  
47  
48  
49  
50

51 The close association among folds, faults and thrusts as well as their cross-cutting  
52 relationships clearly indicates their belonging to flower structures, as suggested by the  
53 close parallelism between the strikes of F2 fold axes and related axial planes with the  
54 strike of thrusts and faults. All these structures can be regarded as related to the NAFZ  
55 system.  
56  
57  
58  
59  
60  
61  
62  
63  
64  
65

1  
2  
3  
4 The structural setting of the Tarakli Flysch identified in the field can be also  
5 recognized in a N-S trending geological cross-section of the Boyali area reported in Fig.2.  
6 In this cross-section, asymmetric flower structures can be identified, even if the  
7 distribution of these structures is not homogeneous. Along the cross-section, the southern  
8 contact of the Tarakli Flysch with the Eocene deposits corresponds to a dextral high-angle  
9 fault whereas, at the northern edge of the cross-section, the Tarakli Flysch is separated  
10 from the IPS units by a low-angle thrust (Fig.2).  
11  
12  
13  
14  
15  
16  
17

#### 18 **4. Discussion**

19  
20

21 The succession of the Tarakli Flysch cropping out in the Boyali area shows a clear  
22 thickening and coarsening upward evolution from thin-bedded turbidites to medium-  
23 grained arenites and calcareous coarse-grained turbidite lithofacies. This succession ends  
24 with a level of slide-block in shaly-matrix lithofacies, that can be considered as the fast  
25 catastrophic event that predates the closure of the basin and its deformation. This  
26 evolution is typical of syn-tectonic sedimentation in a foredeep environment as detected,  
27 for instance, for the Pindos Flysch (Bortolotti et al., 2009).  
28  
29  
30  
31

32 The nanofossil analyses indicate an Early Maastrichtian age for the lowmost level of  
33 the studied succession, whereas a Middle Paleocene age can be proposed for its top, i.e.  
34 the slide-block in shaly-matrix lithofacies.  
35  
36

37 The arenite composition indicate that the foredeep basin is filled mainly by sediments  
38 derived from a source area, related to the IZ Terrane, according to lithic fragments in the  
39 arenites debris and the composition of the main slide-blocks in the uppermost part of the  
40 succession. This conclusion is confirmed by the finding of blocks of ortho- and  
41 paragneisses and amphibolites resembling the pre-Cambrian basement of the IZ Terrane  
42 together with the blocks of Ordovician quartz-arenites, Silurian black shales and  
43 Devonian-Carboniferous limestones of Upper Paleozoic age, which are only observed in  
44 the IZ Terrane in NW Anatolia (Yanev et al, 2006). The IZ Terrane was probably thrust  
45 over the IPS ophiolites and m $\grave{e}$ lange, that only rarely provided debris, according to the  
46 occurrence of scattered block of serpentinites in the youngest lithofacies.  
47  
48  
49  
50  
51  
52  
53

54 The D1 deformation can be regarded as the result of the emplacement over the Tarakli  
55 Flysch of the IZ Terrane with the IPS ophiolites and m $\grave{e}$ lange at its base. The age of the  
56 D1 phase can be thus bracketed between the Middle Paleocene, i.e. the age of the  
57 youngest deposits involved in the deformation and the Early Eocene (NP 14, our  
58  
59  
60  
61  
62  
63  
64  
65

1  
2  
3  
4 unpublished data), i.e. the age of the oldest deposits unconformably overlying the Tarakli  
5 Flysch as well as the overlying tectonic units.  
6

7  
8 The structures of the D2 phase can be instead regarded as related to the flower  
9 structures developed during the transpressional tectonics connected with the NAFZ  
10 system. Therefore, if the inception of the NAFZ activity has been generally regarded as  
11 Miocene (e.g. Bozkurt, 2001), a same age can be assigned to the D2 structures in the  
12 Tarakli Flysch.  
13  
14  
15

## 16 17 18 **5. Conclusions** 19

20  
21 The Tarakli Flysch in the Boyali area can be interpreted as an Early Maastrichtian-  
22 Paleocene turbidite and mass-gravity deposits sedimented in a foredeep basin. The  
23 substratum of this basin was represented by the SK Terrane whereas its northern edge  
24 was constituted by a mobile belt, that, according to arenite and slide blocks composition,  
25 was represented by the IZ Terrane thrust over the IPS units. The latters provide scattered  
26 slide bloks of serpentinites found only in the uppermost levels of the Tarakli Flysch. This  
27 basin was developed during the final stage of the closure of the IPS zone as result of the  
28 progressive convergence between SK and Eurasia plates. After the Middle Paleocene, but  
29 before the Early Eocene, the D1 deformation phase can be regarded as the signal of final  
30 emplacement of the IZ Terrane and the IPS units zones over the foredeep basin where  
31 the Tarakli Flysch sedimented. The structure originated during this event are sealed by  
32 Early Eocene deposits and strongly reworked by the NAFZ tectonics starting from the  
33 Miocene time when the Tarakli Flysch was affected by the D2 phase deformation.  
34  
35  
36  
37  
38  
39  
40  
41  
42  
43

## 44 **Acknowledgements** 45

46 The research has been funded by Darius Project (resp. M.Marroni). This research benefits  
47 also by grants from PRIN 2008 project (resp. M.Marroni) and from IGG-CNR. Geology  
48 students Kaan Tekin, Ali Uygur Karabeyoglu and Remziye Ezgi Çakıroglu are thanked  
49 for their assistance in the field.  
50  
51  
52  
53  
54  
55  
56  
57  
58  
59  
60  
61  
62  
63  
64  
65

## References

- Bojar Melinte, A.V., Dobrinescu, M.C., Bojard H.P., 2009. A continuous Cretaceous-Paleocene red bed section in the Romanian Carpathians. In: Cretaceous Oceanic red beds: stratigraphy, composition, origins, paleoceanographic and paleoclimatic significance. SEPM Special Publication 91, 121-144.
- Bown, P.R., 1999. Calcareous Nannofossil Biostratigraphy. In: P.R., Bown (Ed.), British Micropaleontological Society Publications series, Kluwer Academic Publishers, pp. 314.
- Bortolotti, V., Carras, N., Chiari, M., Fazzuoli, M., Marcucci, M., Nirta, G., Principi, G., Saccani, E., 2009. The ophiolite-bearing mélangé in the Early Tertiary Pindos Flysch of Etolia (Central Greece). *Ofioliti* 34(2), 83-94.
- Bozkurt, E., 2001. Neotectonics of Turkey – a synthesis. *Geodinamica Acta* 14(1-3), 3-30.
- Bralower, T.J., Monechi, S., Thierstein, H.R., 1989. Calcareous Nannofossil zonations of the Jurassic-Cretaceous boundary interval and correlation with the geomagnetic polarity timescale. *Marine Micropaleontology* 14, 153-235.
- Dizer, A., Meriç, E., 1983. Late Cretaceous-Paleocene stratigraphy in northwest Anatolia. *Maden Tetkik ve Arama Enstitüsü Dergisi* 95/96, 149–163.
- Göncüoğlu, M.C., Dirik, K., Kozlu, H., 1997. General Characteristics of pre-Alpine and Alpine Terranes in Turkey: Explanatory notes to the terrane map of Turkey. *Annales Géologique de Pays Hellenique, Geol.Soc Greece* 37, 515-536.
- Göncüoğlu, M.C., Gursu, S., Tekin, U.K., Köksal, S., 2008. New data on the evolution of the Neotethyan oceanic branches in Turkey: Late Jurassic ridge spreading in the Intra-Pontide branch. *Ofioliti* 33, 153-164.
- Gorur, N., Monod, O., Okay, A.I., Sengör, A.M.C., Tuysuz, O., Yigitbas, E., Sakinc, M., Akkök, R., 1997. Palaeogeographic and tectonic position of the Carboniferous rocks of the western Pontides (Turkey) in the frame of the Variscan belt. *Bulletin de la Société Géologique de France* 168, 197–205.
- Martini, E., 1971. Standard Tertiary and Quaternary calcareous nannoplankton zonations. In: *Proceedings of the Second Planktonic Conference Rome 1970*, A., Farinacci (Ed.). Edizioni Tecnoscienza 2, 739-785.
- Okay, A.I. & Göncüoğlu, M.C., 2004. The Karakaya Complex: A Review of Data and Concepts. *Turkish Journal of Earth Science* 13, 77-95.
- Okay, A.I., Monod, O., Monié P., 2002. Triassic blueschists and eclogites from northwest Turkey: vestiges of the Paleo-Tethyan subduction. *Lithos* 64, 155–178.
- Perch-Nielsen, K., 1985a. Mesozoic calcareous nannofossils. In: H.C., Bolli, J.B., Saunders, K., Perch-Nielsen (Eds.), *Plankton Stratigraphy*, Cambridge University Press, pp. 329-426.

- 1  
2  
3  
4 Perch-Nielsen, K., 1985b. Cenozoic calcareous nannofossils. In: H.C., Bolli, J.B., Saunders, K.,  
5 Perch-Nielsen (Eds.), *Plankton Stratigraphy*, Cambridge University Press, pp. 427-554.  
6  
7 Robertson, A.H.F., Ustaömer, T., 2004. Tectonic evolution of the Intra-Pontide suture zone in the  
8 Armutlu Peninsula, NW Turkey. *Tectonophysics*, 381: 175-209.  
9  
10 Roth, P. H., Medd, A. W., Watkins, D. K., 1983. Jurassic calcareous nannofossil zonation, an  
11 overview with new evidence from Deep Sea Drilling Project Site 534. In Gradstein, F.,  
12 Sheridan, R., et al., *Init. Repts. DSDP, 76*, Washington (U.S. Govt. Printing Office), pp. 573-  
13 579.  
14  
15  
16 Saribudak, M., Sanver, M., Ponat, E., 1989. Location of western Pontides, NW Turkey, during  
17 Triassic time: Preliminary palaeomagnetic results. *Geophysical Journal* 96, 43–50.  
18  
19 Sayit, K., Göncüoğlu, M.C., 2009. Geochemical characteristics of the basic volcanic rocks within  
20 the Karakaya Complex: a review. *Yerbilimleri* 30, 181–191  
21  
22 Ustaömer, P.A., Rogers G., 1999. The Bolu Massif: remnant of a pre-Early Ordovician active  
23 margin in the west Pontides, northern Turkey. *Geological Magazine* 136 (5), 579-592.  
24  
25 Yanev, S., Göncüoğlu, M.C., Gedik I., Lakova, I., Boncheva, I., Sachanski, V., Okuyucu, C., Özgül,  
26 N., Timur, E., Maliakov, Y., Saydam, G., 2006. Stratigraphy, correlations and palaeogeography  
27 of Palaeozoic terranes in Bulgaria and NW Turkey: A review of recent data. In: Robertson, AHF,  
28 Mountrakis, D., (Eds) ,*Tectonic development of the Eastern Meditteranean Region*, Geol. Soc.  
29 London Spec. Publ. 260, pp 51-67.  
30  
31 Yigitbas, E., Elmas A., Yılmaz Y., 1999. Pre-Cenozoic tectonostratigraphic components of the  
32 western Pontides and their geological evolution. *Geological Journal* 34, 55-74  
33  
34 Zuffa, G.G., 1980. Hybrid arenites: their composition and classification. *Jour. Sed. Petrol.* 50, 21-29.  
35  
36 Zuffa, G.G., 1987. Unravelling hinterland and offshore paleogeography from deepwater arenites.  
37  
38 In: Leggett, J.K., Zuffa, G.G., (Eds.), *Marine Clastic Sedimentology: Concepts and Case*  
39 *Studies*, London, Graham & Trotman, pp. 39-61.  
40  
41  
42  
43  
44  
45  
46  
47  
48  
49  
50  
51  
52  
53  
54  
55  
56  
57  
58  
59  
60  
61  
62  
63  
64  
65

1  
2  
3  
4 **FIGURE CAPTIONS**  
5  
6  
7

8 Fig. 1 *column* Fig. 1. A) The major tectonic zones of Turkey separated by sutures (modified from Sengör  
9 and Yılmaz 1981). B) Tectonic sketch of the Bayramoren-Arac area. 1) Alluvial deposits; 2) Pliocene  
10 deposits; 3) Eocene deposits; 4) IZ Terrane; 5) IP Suture Zone, Low-Grade Metamorphic Unit; 6) IP Suture  
11 Zone, High-Grade Metamorphic Unit; 7) IP Suture Zone, Ophiolitic Units; 8) IP Suture Zone, Arkotdag  
12 Mèlange; 9) SK Terrane.  
13

14 Fig. 2. *whole page* A) Geological-structural map of the study area. 1) Alluvial deposits; 2) Pliocene  
15 deposits; 3) Middle Eocene deposits; 4) Lower Eocene deposits; 5) Low-Grade Metamorphic Unit; 6)  
16 Arkotdag Mèlange; 7) Basalts; 8) Tarakli Flysch, slide-block in shaly-matrix; 9) Tarakli Flysch,  
17 orthoconglomerates; 10) Tarakli Flysch, thin-bedded turbidites; 11) Jurassic-Cretaceous limestones; 12)  
18 Granites; 13) Cataclastic zones; 14) Main strike-slip faults; 15) Main faults; 16) Thrust faults; 17)  
19 Stratigraphic boundaries; 18) Bedding; 19) Vertical bedding; 20) AP1 axial plane; 21) vertical AP1 axial  
20 plane; 22) AP2 axial plane, 23) A1 fold axes; 24) A2 fold axes with vergence; 25) Horizontal A2 fold axes;  
21 26) High-angle strike-slip faults; 27) Low-angle thrust faults; 28) Location of sampled sites for  
22 nannoplankton analyses; 29) Trace of the geological cross-section. B) Geological cross-section.  
23

24 Fig. 3 *whole page* Stratigraphy and petrographic features of the Tarakli Flysch. A) Reconstructed  
25 stratigraphic log of the Tarakli Flysch. The position of the studied samples are indicated in the left side of  
26 the log. Lithofacies legend: 1 - slide-block in shaly-matrix; 2 - calcareous coarse-grained turbidites; 3 -  
27 conglomerates; 4 - medium-grained arenites; 5 - thin-bedded turbidites. B) field occurrence of the Tarakli  
28 Flysch in the Boyali area. 1 - TBT lithofacies; 2 - uppermost part of the TBT lithofacies, the circle indicate  
29 decimetric lenticular beds of coarse-grained arenites sampled for arenites petrography (sample TC 188); 3 -  
30 dm-thick level of well rounded to matrix-supported conglomerates, Boyali village area; 4 - huge slide-  
31 blocks of quartzarenites (sample TC 37) embedded in a fine grained-matrix shaly matrix (Boyalıçay  
32 Valley); 5 - slide-blocks of crinoidal Devonian-Carboniferous limestones (Boyalıçay Valley); 6 -  
33 photomicrographs of mixed/hybrid siliciclastic-carbonate petrofacies typical of the Tarakli Flysch arenites.  
34 Black arrow indicates an extrabasinal carbonate fragment (oolitic grainstone) while the white arrow  
35 indicates a coeval carbonate intrabasinal fragment (micritized bivalve fragment), sample TC201. C)  
36 Ternary plots showing framework modes of arenites from Tarakli Flysch plotted on: NCE CI+NCI CE  
37 (Zuffa, 1980); Q F L+C (Dickinson, 1985); Lm Lv Ls+c (Ingersoll and Suczek, 1979).  
38

39 Fig.4 *whole page* Examples of deformation structures in the Tarakli Flysch. A: Interference between F1 and  
40 F2 folding; AP1: F1 axial plane; AP2: F2 axial plane. B: Folds associated with strike-slip faults; S1: traces  
41 of bedding. C: Asymmetric F2 folds associated with low angle thrust faults. D: Stereograms of structural  
42 elements; Equal area projection, lower hemisphere.  
43  
44  
45  
46  
47  
48  
49  
50  
51  
52  
53  
54  
55  
56  
57  
58  
59  
60  
61  
62  
63  
64  
65

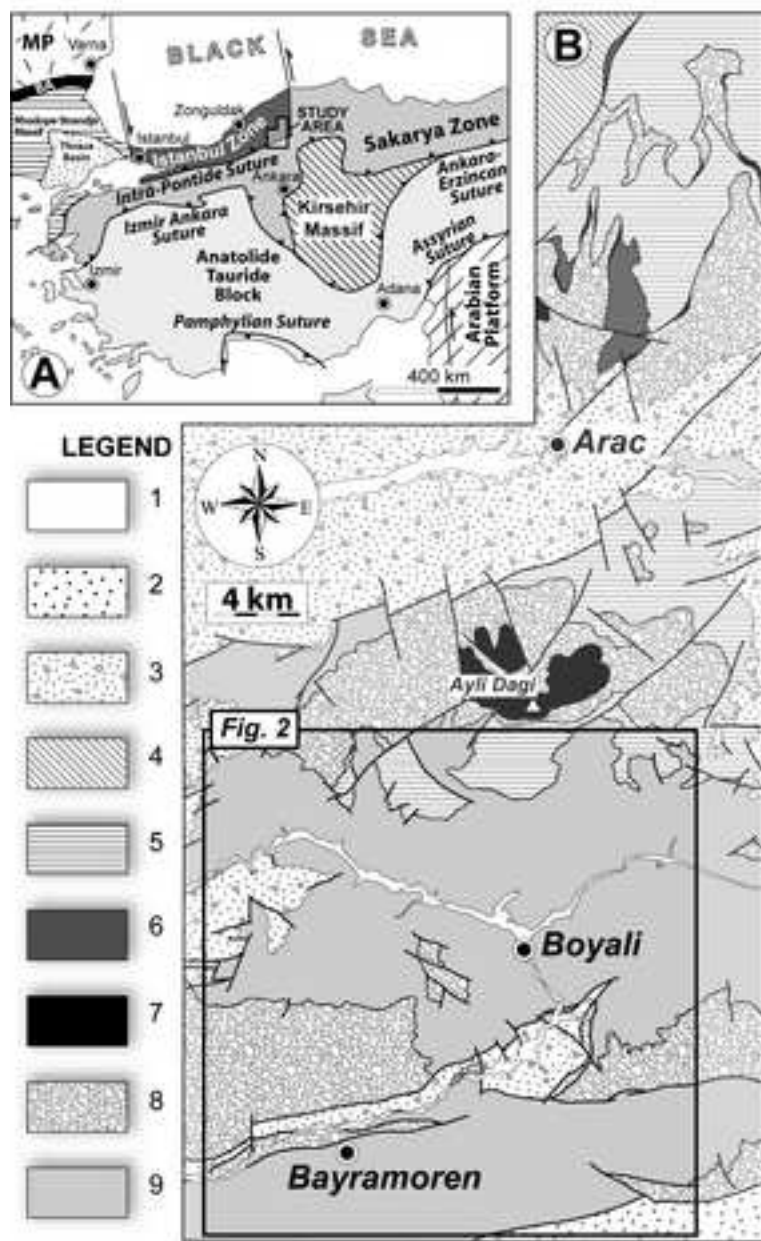




Figure (pas au format Adobe Illustrator / Not Adobe Illustrator file)  
[Click here to download high resolution image](#)

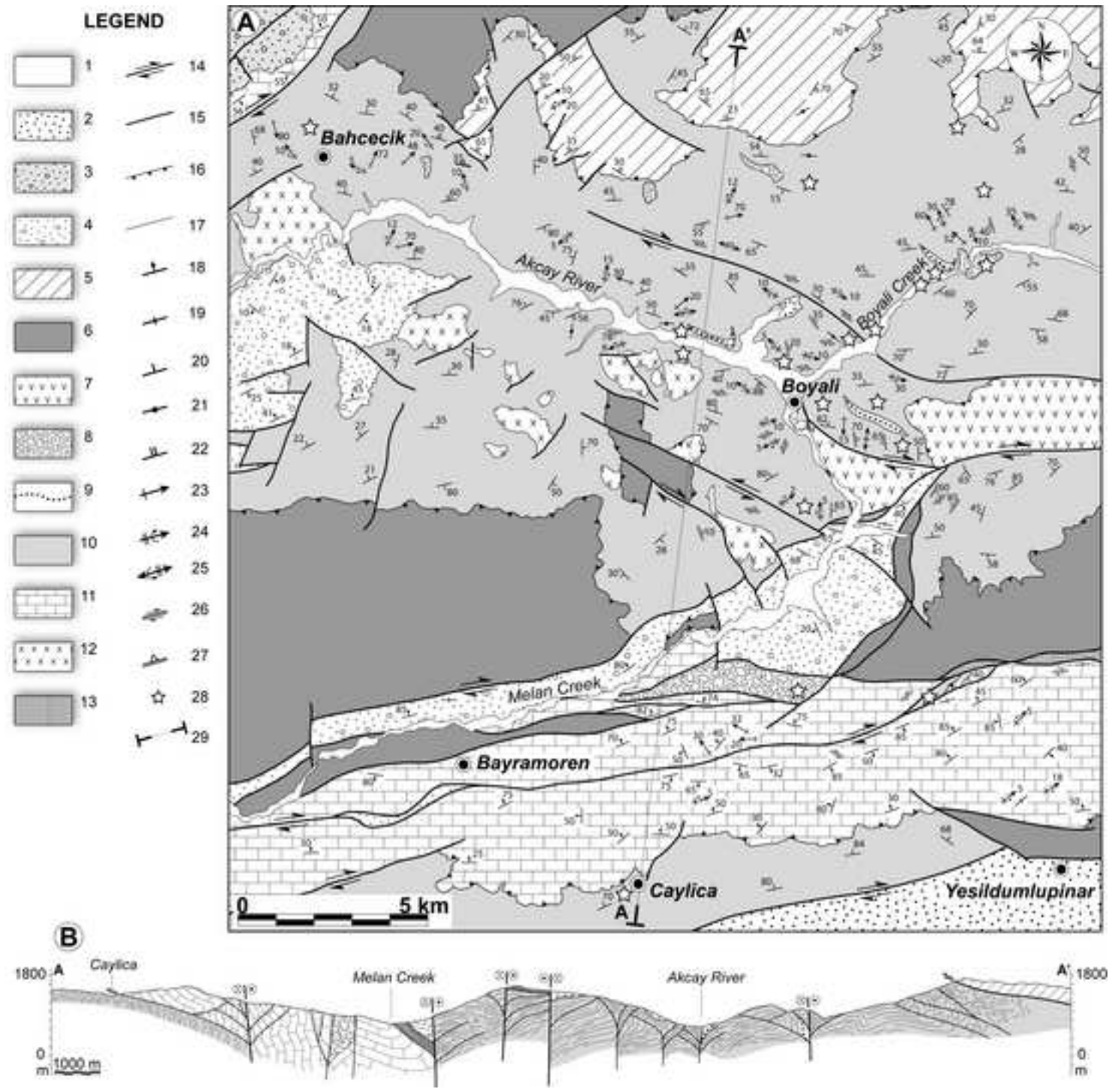


Figure (pas au format Adobe Illustrator / Not Adobe Illustrator file)  
[Click here to download high resolution image](#)

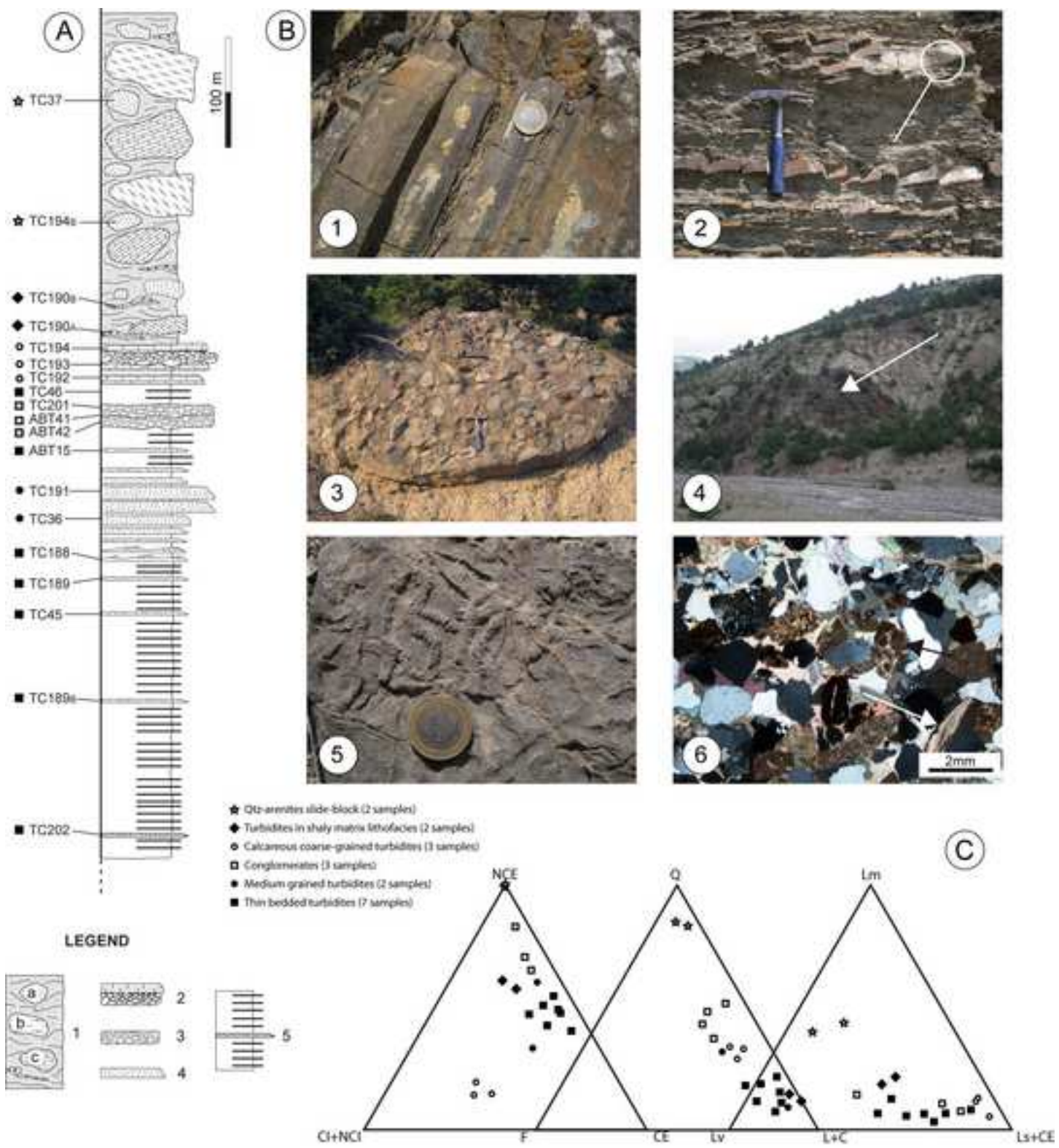


Figure (pas au format Adobe Illustrator / Not Adobe Illustrator file)  
[Click here to download high resolution image](#)

